Flexible and Printed
Electronics



# Improving solder wettability atop screen-printed copper for flexible hybrid electronic circuit assembly

# Improving solder wettability atop screen-printed copper for flexible hybrid electronic circuit assembly

**François-Xavier Fortier[1], Luis-Felipe Gerlein[1], Jaime Benavides-Guerrero[1], Arjun Wadhwa[1], Krunal Shah[1], Mohamad Hassan Taherian[2] Alexandre Perrotton[1], Martin Bolduc[2] and Sylvain G. Cloutier[1]**

[1] Department of Electrical Engineering, École de technologie supérieure, Montréal, Québec, Canada

[2] Department of Mechanical Engineering, Université du Québec à Trois-Rivières, Trois-Rivières, Québec, Canada

E-mail: `sylvaing.cloutier@etsmtl.ca`

September 2025

**Abstract.**
Poor wettability of solder paste on printed copper (Cu) surfaces presents a significant limitation towards the reliable assembly of flexible hybrid electronic (FHE) circuits. This work addresses this challenge using a low-melting-point, bismuth-based solder on nanoparticle-based copper ink pads serigraphically printed on flexible polyimide. To improve solderability, we introduce a surface treatment involving mechanical polishing of the printed copper with sodium bicarbonate ($NaHCO_{[t]3}$) to reduce surface porosity and remove organic residues. This treatment enhanced solder wettability by 66%, leading to superior component alignment and assembly quality. The fabricated circuits prove highly robust and withstand a 1000-hour accelerated aging test at 85°C and 85% relative humidity. Cross-sectional analysis confirms formation of a $1.5 \pm 0.5\,\mu m$ thick intermetallic layer, indicative of an industrial-quality flexible hybrid electronic circuit.

*Keywords*: Printed Electronics, Flexible Hybrid Electronics, Surface Mount Assembly, Copper Ink, Solder Paste

Submitted to: *Flexible and Printed Electronics*

## 1. Introduction

In the context of printed electronics, efforts are made to fabricate electronic circuits using additive manufacturing techniques [1, 2]. This approach targets lower production costs, reduces waste, and alleviates the use of environmentally harmful chemicals used in traditional circuit manufacturing [2]. However, most integrated circuits (ICs), also known as microchips, can't be printed due to the required precision and level of complexity [1–5]. As a result, flexible hybrid electronics (FHE) design strategies seek to combine complex pre-packaged components with printed circuitry elements [1–7]. Once the circuits are printed, the ICs and other surface-mount devices (SMDs) are usually attached using a conductive adhesive or a solder paste [8–12]. Because FHE circuits are mostly fabricated from low-cost and temperature-sensitive substrates, conductive adhesives are generally used for component attachment to avoid any thermally-induced damage to the substrates [10, 11, 13, 14]. In the FHE literature, the current state-of-the-art discussed in the following section involves epoxy- and/or solder-attachment of SMD components on various types of inks.

### *1.1. State-of-the-art solder assembly on silver prints*

Flexible hybrid electronic (FHE) circuits populated through surface mount assembly (SMA) on printed silver using reflow melting of solder paste have been documented [15, 16]. These assemblies are mostly reported on circuits fabricated using inkjet, dispensing, or serigraphic (screen) printing of silver-based inks [4, 14, 17, 18].

Component (or SMD) shear tests performed to evaluate the strength and integrity of solder joints holding components suggest that the capillary effect of nanoparticle-based inks promotes shear strengths similar to that of silver epoxies and stronger than solder-pasted components [18]. However, shear strength values can vary significantly depending on the substrate type (paper, polyimide, or glass) associated with different capillarity actions between the silver nanoparticle-based inks and these substrates [18].

It is now understood that the surface morphology of the silver-based prints also has a clear impact on the interaction and melting dynamics of the solder paste for SMD assembly, especially on inks deposited by inkjet [17]. This process still requires a solder paste with a peak reflow temperature of 235°C, yielding cracks in the print and the solder leaching of the printed contact pads [17]. This leaching occurs when the melting solder dissolves and absorbs the printed pads from the substrate [17].

Assemblies on inkjet-printed silver are also realized using SnBi, SnBiAg solder pastes and isotropic conductive adhesives (ICAs) [14]. There, reliability tests conclude that the coefficient of thermal expansion also has a clear impact on the SMD adhesion, while using ICAs can yield longer lifetimes [14].

Alternatively, a state-of-the-art nScrypt micro-dispensing system was also used to print both silver conductive ink and a low-melting-point solder together to create functional assemblies [4]. The ability to dispense both materials requires control over the timing of material flow and the position of the valve rod [4]. Interestingly, these results suggest that their solder paste, which has a peak reflow temperature lower than 160°C, was hydrophobic on the silver printed on polyimide substrate, but it still allowed a good wetting on silver prints deposited atop copper-based substrates [4].

### *1.2. Solder assembly on copper prints*

Copper-based inks offer a promising alternative to silver inks for printed electronics, as they can reach the necessary conductivity required for industrial applications and remain compatible with standard processes [19, 20]. Another advantage resides in the fact that copper is roughly 1000 times more abundant than silver [21–24].

A comparative study of solderability on both silver and copper printed inks was published as early as 2008 [25]. These inks consisted of metal powders with high-temperature organic binders. However, the origin, particle sizes, metal purity, or the chemical composition of the organic binders were not mentioned in the article. In this study, silver and copper inks are printed atop rigid FR4, then dipped into Sn-Ag-Cu and Sn-Pb solder baths of unspecified alloy concentrations. While the solder fully covers the printed metal, it still led to a "poor" solderability on both the silver and copper prints. The cross-sectional analysis of the prints suggests poor wetting, which is attributed to surface roughness and heterogeneity [25].

In 2019, screen-printed copper ink was developed from Cu nanoparticles (CuNP) formate [26]. Intermetallic bonds were formed between this ink and the SAC305 solder paste. However, the assembly is only achieved using a reflow oven on a print containing only CuNP and the binder. While the solder wetting of the CuNP prints is not quantified, the authors conclude with an emphasis on the formulation of a solderable screen-printable Cu ink to print fine features and be sintered either thermally or using a flash lamp [26].

Today, achieving reliable surface mount assemblies of electronic components on printed copper circuitry still remains a problem for FHE integration.

### *1.3. Objective of this study*

As a result, FHE circuits are still mostly fabricated using silver-based inks [2]. While affordable copper-based inks were recently developed, it is imperative to develop suitable assembly strategies using standardized equipments and processes. In this work, we achieve SMD component assembly on printed copper circuits by improving the solder wettability between commercial copper ink and solder paste. Indeed, we demonstrate that the melted solder paste does not properly wet the pristine printed copper without any intermediary surface preparation step to improve solder paste wettability. This aspect is essential to allow printed circuits to be assembled using standard assembly line equipment. Another important aspect of this research is to replace the silver with copper prints to alleviate significant electro-migration issues associated with silver [27].

As shown in Figure 1, it is clear that the solder paste can't properly wet the surface of the pristine copper print. There, we compare the wetting on copper prints and on laminated copper sheets with electroless nickel immersion gold electroplating. The solder wetting problem is highlighted in Figure 1(c), where the solder is seen to coalesce to leave most of the printed copper surface exposed. In Figure 1(d), solder spreads on the electronic component pads. These results clearly emphasize the need for further investigation to improve the solder wetting on the copper prints and achieve more robust and reliable solder joints.

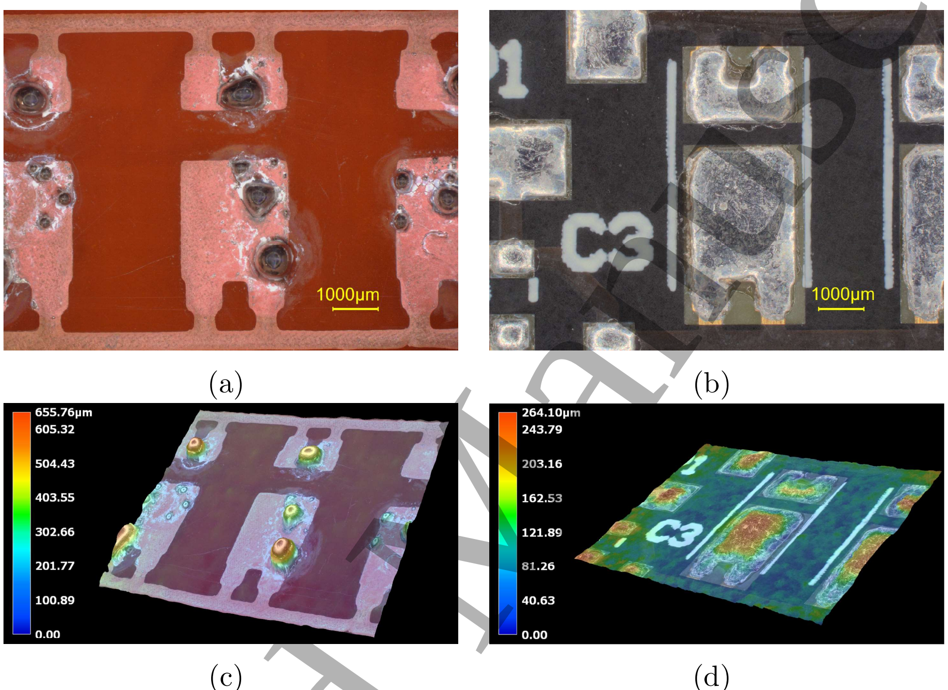


Figure 1: Solder wetting on different types of circuits. (**a**) Melted solder paste on a circuit printed with LF360 copper ink. (**b**) Melted solder paste on a commercial circuit made from copper laminate. (**c**) 3D topographic representation of the melted solder on the copper print seen in (**a**). (**d**) 3D topographic representation of the circuit seen in (**b**).

## 2. Materials and Methods

### *2.1. Materials*

The circuits are printed on commercial polyimide (PI) sheets from American Durafilm inc. of type 500FPC, (Holliston, USA) with a 127 $\mu m$ (5 mils) thickness using the commercial copper ink LF360 from Copprint (Jerusalem, Israel). The prints are prepared using a serigraphic Keko P200S printer using a silk mesh with 280 meshes per inch square. The printed ink is then dried for 2 minutes at 90°C before sintering at 300°C using a laminator. As for the solder paste, a paste with low melting point is selected to avoid deformations and creeping in the PI substrate. We use the Indium5.7LT-1 Indalloy®281 (58 Bi/42 Sn) from Indium Corporation® (Clinton, USA). Furthermore, the solder paste used for the experiments is type 4. The circuit design for the experiment included the footprint of the Seoul Semiconductor LED STW8Q14D (Ansan-si, Korea).

### *2.2. Surface Treatment Methods*

Three surface treatments are explored. The first surface treatment involves immersion of the circuit in 10% acetic acid solution for 20 seconds. Then, the circuit is wiped off with a piece of lint-free cloth until dry. This is meant to remove the copper oxide layer from the print and provide a copper-rich surface for soldering [28]. For the second surface treatment, polishing of the surface is aimed to completely remove the upper layer of the print. To perform the polishing, non-toxic sodium bicarbonate is used. The sodium bicarbonate is sourced in powder form, pure, and from a conventional retailer. The prints are rubbed with the sodium bicarbonate until the surface achieves a bright copper finish. The third and last surface treatment repeats the same procedure as in the second, but finishes with an immersion in acetic acid for 20 seconds.

### *2.3. Solder Wetting Quantification Method by % Coverage estimation*

The Ilastik segmentation toolkit is used to quantify the surface covered by the solder paste on the print [29]. The segmentation training considers drawing some reference segments to distinguish each of the areas of interest for the algorithm to learn properly. Then, the software can process the images of the printed samples, yielding a colored-segmented image where the exposed copper is clearly distinguishable from the parts covered with solder paste. These resulting images are exported in binary 8-bit grayscale format so that the coverage ratio can be calculated as a percentage (% ). This last step is performed using ImageJ to extract the pixel count for each level of gray from the image.

## 3. Results

### *3.1. Surface Analysis*

A micrograph analysis of the surface in obtained under scanning electron microscope (SEM) and shown in Figure 2. In Figure 2(a), the low-resolution image shows a somewhat uniform surface with some porosity. In Figure 2(b), the higher-resolution image shows the aggregate of copper particles forming the printed surface structure. The particle diameters in Figure 2(b) were measured using ImageJ and the measurements are available in the supplementary information section. The bimodal distribution shows smaller particles with a diameter of $0.18{\pm}0.05$ $\mu m$ and larger particles with a $0.91{\pm}0.16$ $\mu m$ diameter. As expected, Figure 2(b) also suggests that the copper particles have partially sintered together. This implies a residual surface granularity specific to the particle-based ink compared to the smooth surface from a traditional PCB using rolled copper foil laminated on the fiberglass substrate [30].

X-Ray photoelectron spectroscopy (XPS) measurements are performed on the copper prints and the results are shown in Figure 2(c). XPS is a technique where the observed material is irradiated by a beam of X-rays. The material reacts to the exposure by photo-emitting electrons, and their kinetic energy (ejection velocity) is measured. Then, the irradiation energy is subtracted from that value to obtain the binding energy, which depends on the mass of the atomic nucleus and thus the exposed element. This technique can be paired with an ion-beam etching to determine the chemical composition in depth. Also, the XPS measurements require a vacuum to operate [31, 32].

The graph shows the different percentages of chemical elements as a function of their depth depending on the print's surface. Results suggest that the first 100 nm consists primarily of carbon- and oxide-based compounds. As observed, a depth of 500 nm below the surface must be reached before the presence of copper increases to more than 30%.

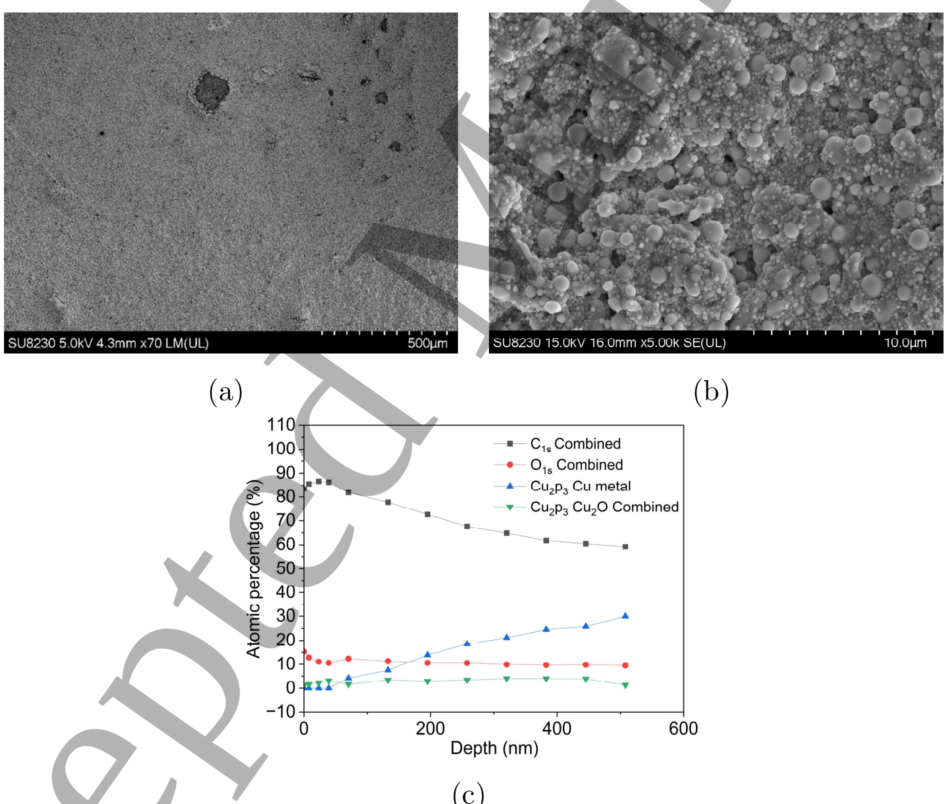


Figure 2: Surface morphology and XPS analysis of the copper prints. (**a**) Low-resolution SEM micrograph of the printed copper surface using a 500 $\mu m$ scale. (**b**) Higher-resolution SEM micrograph of the printed copper surface at 10 $\mu m$ scale. (**c**) XPS analysis of the printed copper surface.

### *3.2. Surface analysis post surface treatment*

Since the appearance of the print changes after sintering, and the XPS analysis indicates a high carbon content in the print's surface, one can reasonably expect sintering residues to carbonize during the thermal treatment. By removing a micron or two of the print surface, the concentration of copper has increased. Indeed, XPS analysis shows that the percentage of copper is higher past 500 nm and that the percentage is extrapolated to increase as it goes deeper into the print.

Figure 3(a,b) shows scanning micrographs taken before and after the sodium bicarbonate surface treatment. The consequences of the treatment on the surface morphology are clearly seen in Figure 3(b), as it shows several areas free of spherical copper particles. These sporadic flat areas are encircled on the micrograph.

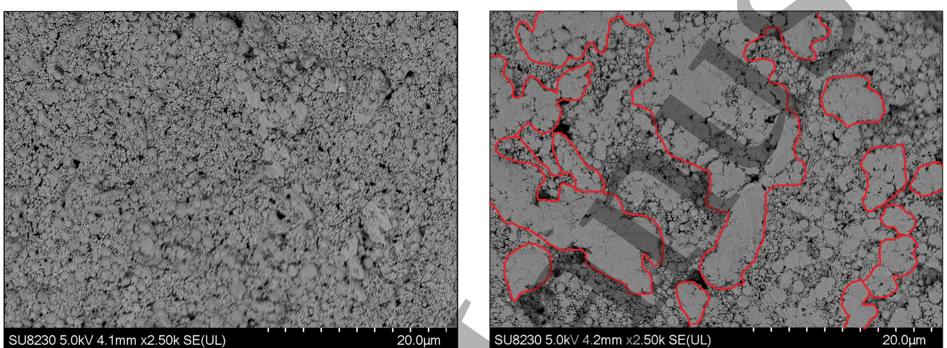


(a) (b)

Figure 3: Schematic representation of the printed copper morphology and SEM micrographs. (**a**) SEM micrograph of the printed copper using a 20 $\mu m$ scale bars. (**b**) SEM micrograph of the printed copper after treatment.

The XPS results shown in Figure 4 reveal the effect of the surface treatments using acetic acid immersion and sodium bicarbonate polishing on the surface composition. Results for the copper print treated with acetic acid suggest a greater copper ratio near the surface compared to untreated circuits. Also, the percentage of carbon-based molecules decreases at a higher rate compared to an untreated circuit. However, the percentages of oxides remain essentially similar.

Meanwhile, Figure 4(b) shows the analysis after a sodium bicarbonate polishing. The initial proportion of carbon compounds decreases from over 60% to approximately 15% within the first 20 nm beneath the surface. Also, the ratio of oxides drops close to zero at 100 nm under the surface. Furthermore, the copper concentration increases at a higher rate compared to the acetic acid treatment. Within 200 nm of the surface, the polished print shows close to 90% of exposed copper, while the acid-treated print reaches such percentages at approximately 600 nm depth beneath the surface. This suggests that the polishing has a clear impact on the surface composition by exposing the metallic copper and removing the excess of carbon-based contaminants.

The last XPS analysis shown in Figure 4(c) is performed on a print polished with sodium bicarbonate, followed by cleaning with acetic acid. The concentration of copper shows a similar progression to Figure 4(b), reaching similar copper exposure percentages. However, the initial ratio of carbon molecules is higher than both the acetic acid, and sodium bicarbonate treatments alone. Considering that the only difference is that the sample in Figure 4(c) is cleaned with acetic acid compared to that sample in Figure 4(b), we can safely assume that the source of the excess carbon is the acetic acid itself or a byproduct of its application.

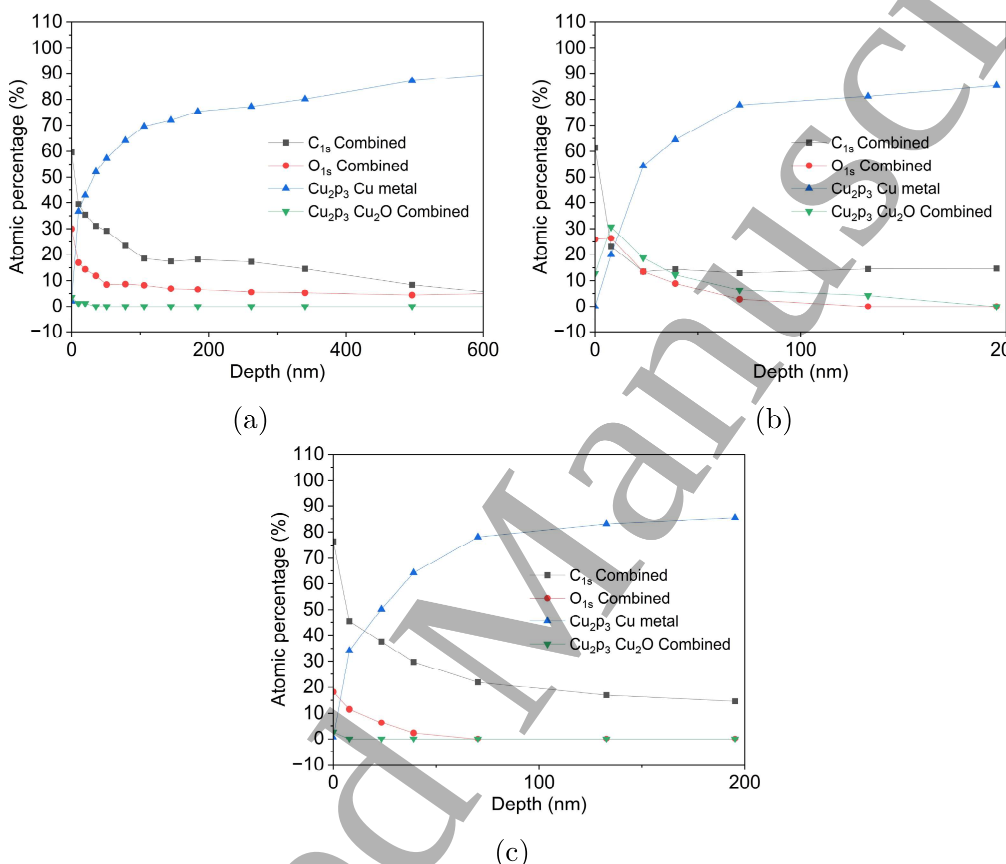


Figure 4: XPS analysis of the printed copper surface after different treatments. (**a**) Chemically treated with acetic acid 10% for 20 seconds. (**b**) Manual surface polishing with sodium bicarbonate. (**c**) Manual surface polishing with sodium bicarbonate, followed by cleaning with acetic acid.

### *3.3. Wetting Coverage Analysis*

In order to quantify the surface wetting improvement, image analysis of LED pads is used to directly evaluate the wetting on the untreated surface, after the acetic acid treatment, after the sodium bicarbonate polishing, and on surfaces treated with both sodium bicarbonate polishing and acetic acid cleaning. High-resolution images are acquired using a Keyence VHX7000 microscope, then segmented with the Ilastik software as described earlier. The segmentation is classified into 3 categories: the solder paste once melted, the copper print, and the PI substrate. If the number of segmented pixels in the copper footprint is zero, this means that the solder paste is wetting 100% of the copper surface. If there are pixels showing the copper, the percentage will be less than

100%. The number of pixels associated with the polyimide is ignored, considering this surface is not part of the assemblies.

Furthermore, Figure 5 shows sets of printed circuits with melted solder for each of the surface treatment strategies. The top part of each sub-figure only presents five (5) of the ten (10) footprints used for solder wetting coverage analysis. Thus, the sample size is ten (10) per surface treatment, and the results are expressed in averages plus or minus their standard deviations. Also, the shear strength results are represented in the same way. The dataset is arranged in this way due to the high resolution of the pictures and the required processing time for each segmentation. The five LED pads were cut from different prints to reduce statistical bias. The entire dataset of all the footprints, their segmentation, and pixel counts is available in the supplementary information section.

The lower part of the LED contact pad is shown in each bottom left corner of the composite sub-figure, while the bottom right sub-figure presents the segmentation results. The segmentation in Figure 5(a) presents a calculated surface coverage of 24.1% , suggesting a solder paste wetting considered phobic. After melting, the paste clumps into bead-like structures. It is important to mention that the print in Figure 5 (a) differs slightly from the prints used for the other wetting tests. This implies that a small gap at the bottom of the footprint is covered by ink instead of being open. After calculating the difference, this correction represents 4% of the printed area and the wetting percentage must be adjusted accordingly. For comparison, the circuit shown in Figure 5 (b) is treated with acetic acid. Segmentation analysis suggests a 60% surface coverage. Figure 5 (c) shows the LED pads that were treated with sodium bicarbonate polishing. By visual observation, the solder paste spreads much more uniformly compared to the acetic acid treatment. This is confirmed by the segmentation analysis suggesting a 90.8% surface coverage. The final solder paste wetting test used a surface previously treated with sodium bicarbonate polishing and acetic acid cleaning. As shown in Figure 5 (d), the resulting segmentation analysis suggests a surface coverage of 85.6%.

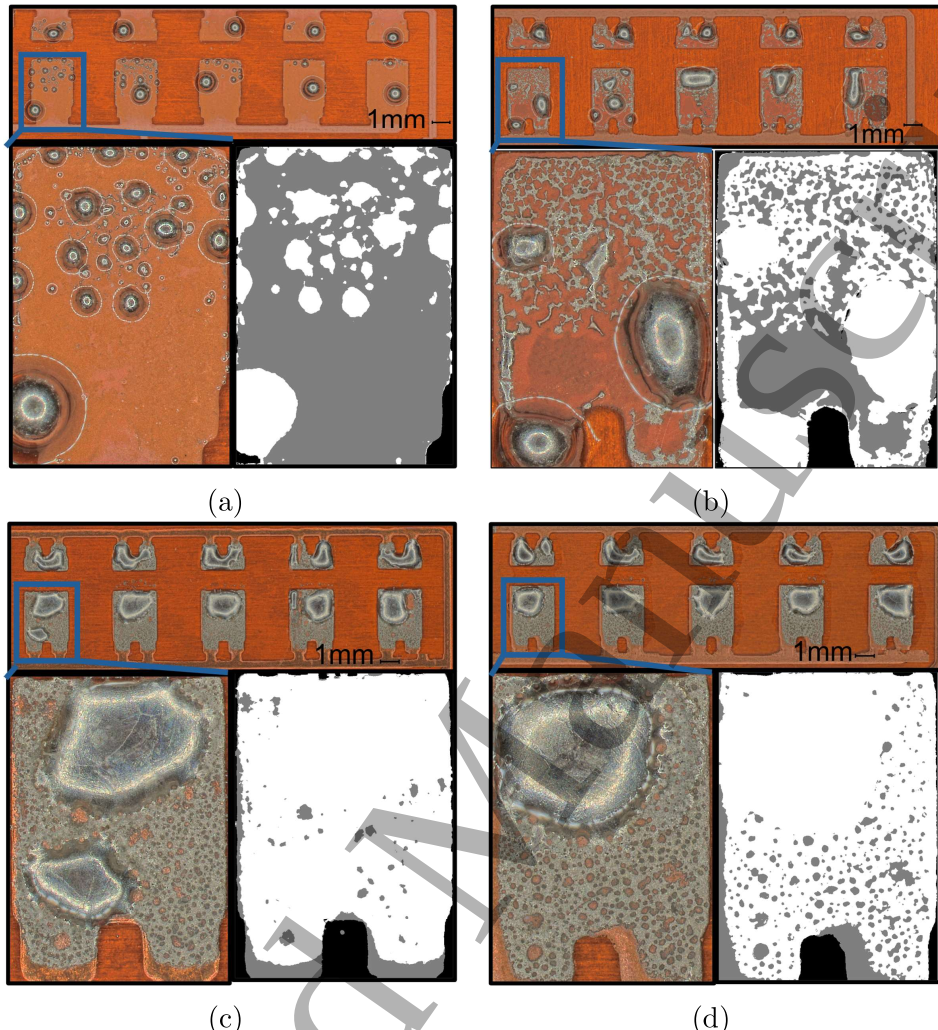


Figure 5: Composite image analysis of solder paste wetting on LED pads after each treatment. (**a**) Control sample showing solder wetting on untreated circuits pads. (**b**) Solder wetting on circuit pads treated with acetic acid for 20 seconds. (**c**) Solder wetting on circuit pads polished using sodium bicarbonate polishing. (**d**) Solder wetting on circuit pads polished using sodium bicarbonate polishing and then treated with acetic acid.

All the surface wetting results for individual samples are presented in the box chart shown in Figure 6. This box chart clearly shows that the sodium bicarbonate treatment and the treatment including an additional acetic acid cleaning achieve the best surface coverages.

According to these results summarized in Table 1, the sodium bicarbonate treatments with and without acetic acid cleaning achieve better wetting than using acetic acid cleaning only. Still, the acetic acid treatment yields a significantly improved coverage compared to the untreated prints. The acceptability threshold set in this research project is a 50% of surface coverage. This choice is consistent with the IPC-A-610G industry standard, which specifies that an SMD assembly must cover at least

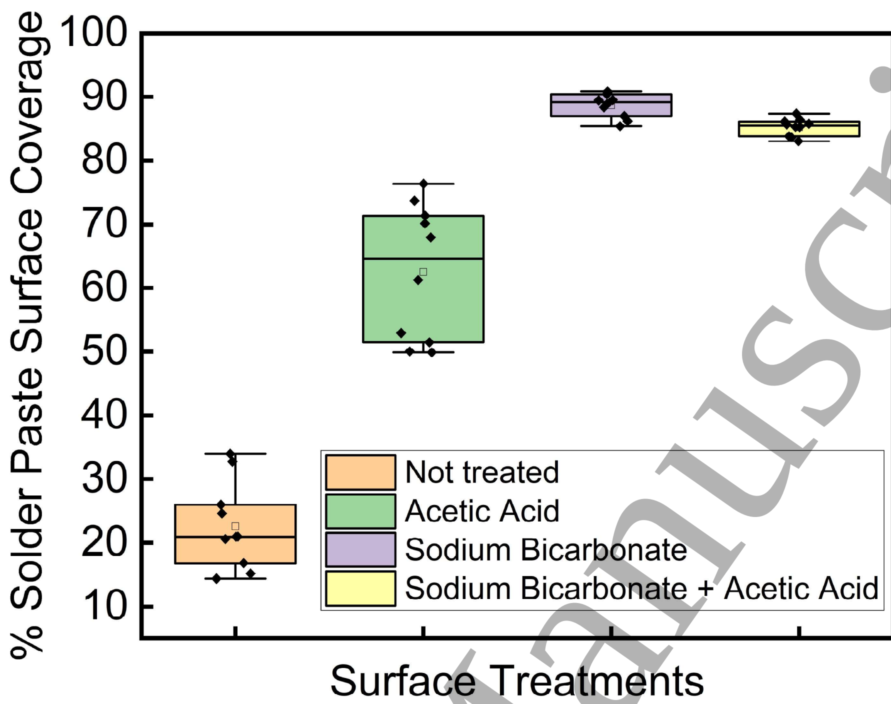


Figure 6: Box chart representation of the solder surface coverage for the ten samples evaluated for each surface treatment protocol.

Table 1: Solder surface wetting results for each applied treatment.

| Surface treatment type | Not treated | Acetic Acid | Sodium Bicarbonate | Sodium Bicarbonate and Acetic Acid |
|---|---|---|---|---|
| Average | 22.6% | 61.3% | 88.9% | 85.3% |
| Median | 21.0% | 60.5% | 89.5% | 85.7% |
| Standard deviation | 6.8% | 11.5% | 2.0% | 1.4% |

50% of the width of the SMD or the pad, whichever is the smallest [33]. According to this criterion, all surface treatments applied to our circuits screen-printed with copper ink are successful.

To assert the results of the solder wetting on the copper prints, pictures of the solder contact angle were taken with a Holmarc HO-IAD-CAM-01B system, and they are available in the supplementary information section. The first picture shows the solder melted on a pristine copper print and the solder has coalesced into a ball atop the print. However, flux resin residue around the melted solder does not clearly show the edge of the ball, and the many attempts to remove it have also wiped out the solder. Knowing the presence of the flux would not give a good profile image, the contact angle was not measured. The second picture presents the melted solder on a copper print polished with sodium bicarbonate. There, the melted solder appears closer to the surface of the circuit as such it "wets" the circuit surface. Furthermore, the contact angle of the melted solder on the treated circuit was measured with ImageJ at 20.8°on the right side and 22.2°on the left side.

### *3.4. Reliability of the assemblies*

For a solder joint to be considered reliable and of good quality, it must form an intermetallic compound (IMC) region [34]. For evaluation, a solder joint was encapsulated in epoxy resin, cross-sectioned, and metallized to perform an electron energy-dispersive spectroscopy (EDS) measurement. The polished cross-section is shown in Figure 7 (a). The cross-sectional SEM micrograph of the solder joint formed after sodium bicarbonate polishing treatment is shown in Figure 7 (b). The particulates from the printed copper ink are visible at the bottom of the figure (high-resolution). The top part of that figure shows the bismuth-tin-based solder in Figure 7 (c). The IMC is easier to observe in Figure 7 (b), where the dark blue hue shows a stoichiometric change, while the EDS imaging of tin in Figure 7(c) shows the presence of tin at this junction. The thickness of the IMC region can be estimated at 1.5±0.5 $\mu m$. This is within the typical IMC thickness values ranging between 1 $\mu m$ to 3 $\mu m$ [35]. To demonstrate the application of this research, Figure 7 (d) shows a functional LED circuit assembled on printed copper circuitry and treated with the sodium bicarbonate polishing before assembly using a conventional reflow oven.

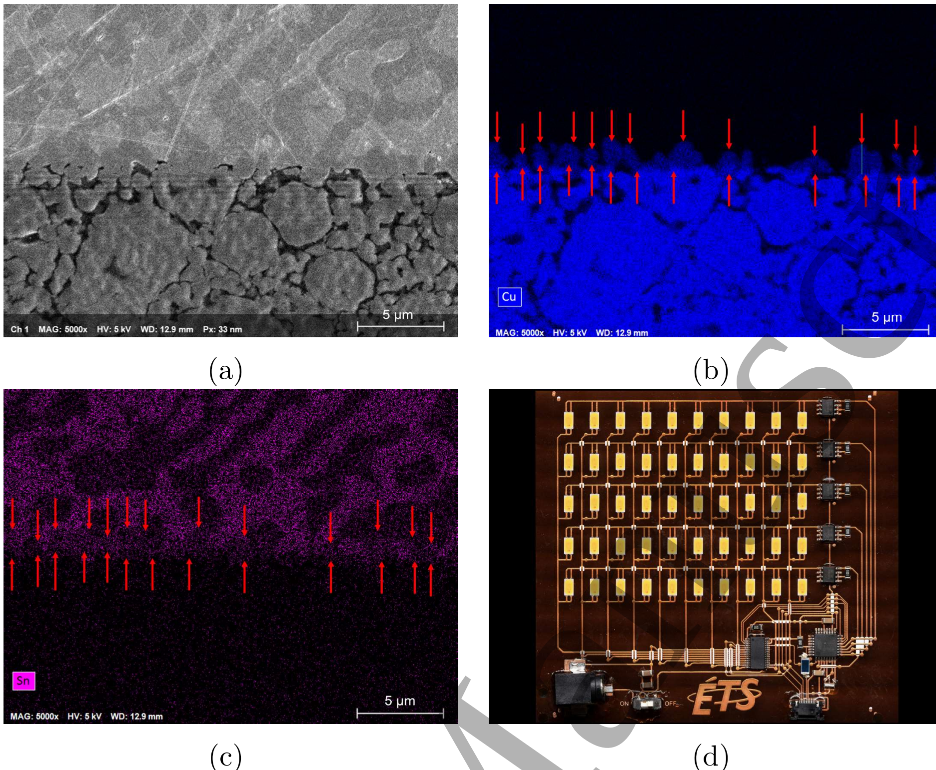


Figure 7: Cross-sectional analysis of a soldered assembly joint formed on a copper print treated with sodium bicarbonate. (**a**) SEM of the cross-sectional assembly solder joint. (**b**) EDS micrograph of the copper present in the assembly. (**c**) EDS micrograph of the tin present in the assembly. (**d**) Printed LED circuit treated with sodium bicarbonate and fully assembled.

The strength of the assembled solder joints was evaluated using a standardized shear test with a calibrated Nordson Dage 4000plus. After measuring the shearing force required to break 30 components from the assembled circuit, the average shearing strength measured is 5.0$\pm$1.5 kg, resulting in the copper ink peeling-off from the PI substrate before breaking of the solder joint could be reached. Further shear tests done with prints treated with either acetic acid or sodium bicarbonate treatment showed a similar behavior. To improve the ink adhesion on the substrate, the polyimide (PI) substrates were treated before copper printing using a 200W oxygen plasma oven for 5 minutes with a throughput of 20cc/min. These treated polyimide sheets were then used to prepare a new set of prints for component assemblies. After replicating the same shearing test procedure, the plasma-treated substrates yield an average shear strength of 9.4$\pm$2.5 kg. For comparison, assemblies performed on a commercial flexible PCB laminates yield an average shear strength of 12.1$\pm$1.7 kg. All the shear test measurements are available in the supplementary information section. The shear tests performed on printed copper circuits still end with the ink being removed from the PI sheet before the solder joint breaks.

## 4. Discussion

The surface of the printed copper is found to be porous and composed of copper particles with carbon and oxide residues, likely originating from the particles' encapsulating agents. Surface treatment methods are explored to increase the wetting of the solder. One of the methods is a polishing of the surface with sodium bicarbonate to remove surface residues and increase copper concentration. After treatment, the atomic concentration of copper reaches 80% at the surface. The SEM micrograph in Figure 3 (b) shows that the treated surface has several flattened areas of a few microns square. The surface of commercial circuits is either made by electroplating or laminating copper on top of the dielectric material. That surface is made of contiguous, flat, and almost pure copper [36]. Thus, the treatment has both smoothed and increased the copper concentration to the point where areas of the print surface are closer to a commercial laminated PCB.

Three different surface treatments are compared to improve solder wetting. At first, the acetic acid was selected to remove copper oxides and possibly the ink sintering residue. The second surface treatment was intended to expose a higher copper concentration in the print through a polishing process. The choice of the polishing media converged on sodium bicarbonate due to its availability, cost, and ease of handling. The idea was to bring the copper print surface closer to a PCB copper laminate, which is known to be compatible with solder paste. In order to obtain a quantitative assessment, a deep machine-learning segmentation algorithm is used to segment photographs and thus differentiate the substrate, the printed copper and the melted solder paste.

The untreated surface, where the paste doesn't wet the surface, yields an average of 22.6% coverage on ten samples. In comparison, surface treatments using acetic acid, sodium bicarbonate alone, and sodium bicarbonate followed with a cleaning with acetic acid give an average surface coverage of 65.7%, 88.9%, and 84.9% respectively, suggesting adequate solder paste wetting. These solder wetting results and XPS analysis show the acetic acid has an impact on removing the copper oxides and sintering residues off the print. Meanwhile, the sodium bicarbonate treatment relies on the abrasion of the surface instead of the chemical reaction achieved with acetic acid. Indeed, sodium bicarbonate is a crystalline salt known to be used to polish silverware [37]. This is supported by the SEM images of the print's surface before and after the sodium bicarbonate polishing, which show flat areas. The surface polishing has given better wetting results than the acetic acid treatment. This is explained by the higher copper concentration achieved through polishing rather than chemical treatment with acid. Additionally, comparing the contact angle between the melted solder on pristine prints and those treated with sodium carbonate shows the improvement achieved by surface polishing.

This research is supported by a paper published in 2008, which claims that the poor wetting is due to the print's coarse and heterogeneous surface. Also, it mentions that the solder wetting could be improved on the copper print if the heterogeneity could be improved. The SEM cross-section analysis presents more voids than those presented in this research [25]. In a study published in 2019, a CuNP and polymer-based ink allowed the formation of an intermetallic junction with SAC 305 solder paste. However, the solder wetting is not quantified, only mentioned as forming a"good" solder joint and withstanding a tape adhesion test [26].

Furthermore, the results from the shear tests show the rupture point is between the ink and the PI substrate, and not between the component and the copper pad. Copper ink adhesion is improved by using oxygen plasma treatment of the substrate, resulting in shear test performances close to those of a commercial flexible PCB circuit.

Also, EDS analysis shows that the IMC has a thickness of about 1.5±0.5 $\mu m$. The presence of an IMC is indicative that the assembly has an alloyed link between the print and the solder, instead of the solder just laying over it. Another improvement in having the solder wet the print surface is the SMD post-assembly placement. As seen in supplementary information, when the solder is phobic on the print, the electronic components often lie atop a solder ball. They are not correctly aligned with their respective footprint.

## 5. Conclusions

In this work, the solder wetting atop a screen-printed copper-based circuit is investigated. A thorough analysis of the printed surface is performed using SEM to reveal the surface morphology and arrangement of the copper particles. XPS measurements indicate the presence of oxides and carbon-based compounds on the copper surface. We establish that improved solder paste wetting can be achieved by treating the surface. Different surface treatments are performed using (1) acetic acid at 10%, (2) manual polishing using sodium bicarbonate, and (3) a combination of both. Each treatment is affordable, free of harmful chemicals, and simple to implement. Once the circuits are treated, the surface analysis shows that the circuits dipped in acetic acid show less oxide residues. Meanwhile, the circuits treated with polishing show diminished carbon and oxide residues within a few hundred nanometers from the surface. As such, the solder paste can be applied and then melted on the treated circuits. After treatment, the surface coverage is quantified with Ilastik learning algorithm and shows increased solder wetting. The highest solder wetting is achieved for the surface treated with sodium bicarbonate alone, followed by the treatment using both. Compared to the untreated copper prints, the solder wetting is increased by 66% when using the sodium bicarbonate treatment. The circuits could be polished by an automated process, either in-line or in batches, using a soda blasting system [38]. Specialized polishing agents could be explored in future studies, and thus possibly optimizing the polishing process. Finally, a good solder-joint assembly is confirmed by the formation of an intermetallic region between the printed copper and the tin-bismuth solder. Also, the surface treatment capability is demonstrated by assembling several ICs of various dimensions, such as a microcontroller and an LED driver. As for the limitation of this study, the observed results are intrinsically linked to the specific interactions between this printed copper ink, its processing, substrate interactions and the solder paste employed.

## 6. Data availability statement

All data that support the findings of this study are included within the article (and any supplementary files).

## 7. Author Contributions

"The circuit printing was performed by L.F. Gerlein, J. Benavides-Guerrero, K. Shah, and M.Hassan Taherian. The circuit drying and curing was performed by A. Wadhwa, L.F. Gerlein, J. Benavides-Guerrero, K. Shah and M.Hassan Taherian. Surface treatments, components, and circuit assemblies were performed by F.X. Fortier. J. Benavides-Guerrero performed the XPS measurements, while SEM and EDS measurements were performed by A. Wadhwa and F.X. Fortier. The wetting coverage assessment, segmentation, and analysis were done by F.X. Fortier and LF. Gerlein. F.X. Fortier and A. Perrotton designed and programmed the LED circuit. S. G. Cloutier and M. Bolduc supervised this work. All authors have read and agreed to the published version of the manuscript."

## 8. Acknowledgments

The authors also thank Mohammad Saadati for performing the EDS and SEM imaging. Lastly, the authors thank Marcel Charest from C2MI for preparing the circuit for the cross-sectional IMC analysis.

## 9. Funding

Sylvain G. Cloutier acknowledges the NSERC-Discovery program (RGPIN 2022-03083) and Canada Research Chair program (CRC-2021-00490) for their financial support.

## 10. Conflict of interest

The authors declare no competing financial interest.

## Bibliography

[1] Zeng X, He P, Hu M, Zhao W, Chen H, Liu L, Sun J and Yang J 2022 *Nanoscale* **14** 16003–16032 ISSN 2040-3364, 2040-3372

[2] Ibrahim N, Akindoyo J O and Mariatti M 2022 *Journal of Science: Advanced Materials and Devices* **7** 100395 ISSN 24682179

[3] Khan Y, Thielens A, Muin S, Ting J, Baumbauer C and Arias A C 2020 *Advanced Materials* **32** 1905279 ISSN 0935-9648, 1521-4095

[4] Lall P, Goyal K, Schulze K and Miller S 2021 Low Temperature Solder Interconnection of Surface Mount Devices with Additively Printed Pads on Flexible Substrate *2021 20th IEEE Intersociety Conference on Thermal and Thermomechanical Phenomena in Electronic Systems (iTherm)* (San Diego, CA, USA: IEEE) pp 972–980 ISBN 978-1-7281-8539-2

[5] Lall P, Narangaparambil J and Miller S 2022 Mechanical and Electrical Properties of Additively Printed Circuits With Magnetically Orientated Anisotropic Conductive Adhesive Attachment for FHE Applications *ASME 2022 International Technical Conference and Exhibition on Packaging and Integration of Electronic and Photonic Microsystems* (Garden Grove, California, USA: American Society of Mechanical Engineers) p V001T03A011 ISBN 978-0-7918-8655-7

[6] Rogers J A, Chen X and Feng X 2020 *Advanced Materials* **32** 1905590 ISSN 0935-9648, 1521-4095

[7] Tong G, Jia Z and Chang J 2018 Flexible Hybrid Electronics: Review and Challenges *2018 IEEE International Symposium on Circuits and Systems (ISCAS)* (Florence: IEEE) pp 1–5 ISBN 978-1-5386-4881-0

[8] Andersson H, Siden J, Skerved V, Li X and Gyllner L 2016 *IEEE Transactions on Components, Packaging and Manufacturing Technology* **6** 478–485 ISSN 2156-3950, 2156-3985

[9] Andersson H A, Manuilskiy A, Haller S, Hummelgård M, Sidén J, Hummelgård C, Olin H and Nilsson H E 2014 *Nanotechnology* **25** 094002 ISSN 0957-4484, 1361-6528

[10] Niittynen J, Kiilunen J, Putaala J, Pekkanen V, Mäntysalo M, Jantunen H and Lupo D 2012 *Microelectronics Reliability* **52** 2709–2715

[11] Putaala J, Hannu J, Kunnari E, Mäntysalo M, Nousiainen O and Jantunen H 2014 *Microelectronics Reliability* **54** 272–280

[12] Pekkanen V, Mäntysalo M, Kaija K, Mansikkamäki P, Kunnari E, Laine K, Niittynen J, Koskinen S, Halonen E and Caglar U 2010 *Microelectronic Engineering* **87** 2382–2390 ISSN 01679317

[13] Lee J, Cho C S and Morris J E 2009 *Microsystem Technologies* **15** 145–149 ISSN 0946-7076, 1432-1858

[14] Jäger J, Buschkamp S, Werum K, Gläser K, Grözinger T, Eberhardt W and Zimmermann A 2022 *IEEE Transactions on Components, Packaging and Manufacturing Technology* **12** 1232–1240 ISSN 2156-3985

[15] Li X, Andersson H, Sidén J and Schön T 2018 *Flexible and Printed Electronics* **3** 015003 ISSN 2058-8585

[16] Silvestre R, Llinares Llopis R, Contat Rodrigo L, Serrano Martínez V, Ferri J and Garcia-Breijo E 2022 *Sensors* **22** ISSN 1424-8220

[17] Juric D, Hammerle S, Glaser K, Eberhardt W and Zimmermann A 2019 *IEEE Transactions on Components, Packaging and Manufacturing Technology* **9** 156–162 ISSN 2156-3950, 2156-3985

[18] Arrese J, Vescio G, Xuriguera E, Medina-Rodriguez B, Cornet A and Cirera A 2017 *Journal of Applied Physics* **121** 104904 ISSN 0021-8979, 1089-7550

[19] Ding S and Tian Y 2019 *RSC Advances* **9** 26961–26980 ISSN 2046-2069 URL `https://xlink.rsc.org/?DOI=C9RA04404C`

[20] Wang Y and Yin Z 2019 *Applied Science and Convergence Technology* **28** 186–193 URL `https://www.e-asct.org/journal/view.html?doi=10.5757/ASCT.2019.28.6.186`

[21] Zhao S, Han F, Li J, Meng X, Huang W, Cao D, Zhang G, Sun R and Wong C P *Small* **14** 1800047 ISSN 1613-6829 URL `https://onlinelibrary.wiley.com/doi/abs/10.1002/smll.201800047`

[22] Li W, Sun Q, Li L, Jiu J, Liu X Y, Kanehara M, Minari T and Suganuma K 2020 *Applied Materials Today* **18** 100451 ISSN 2352-9407 URL `https://linkinghub.elsevier.com/retrieve/pii/S2352940719305694`

[23] Li X, Wang Y, Yin C and Yin Z 2020 *Journal of Materials Chemistry C* **8** 849–872 ISSN 2050-7526, 2050-7534 URL `https://xlink.rsc.org/?DOI=C9TC04744A`

[24] Ravi Kumar D V, Woo K and Moon J 2015 *Nanoscale* **7** 17195–17210 ISSN 2040-3364, 2040-3372 URL `https://xlink.rsc.org/?DOI=C5NR05138J`

[25] Salam B and Lok B 2008 Solderability and reliability of printed electronics *2008 15th International*

*Symposium on the Physical and Failure Analysis of Integrated Circuits* pp 1–4 ISSN 1946-1550 URL https://ieeexplore.ieee.org/document/4588211/

[26] Deore B, Paquet C, Kell A J, Lacelle T, Liu X, Mozenson O, Lopinski G, Brzezina G, Guo C, Lafrenière S and Malenfant P R L 2019 *ACS Applied Materials & Interfaces* **11** 38880–38894 ISSN 1944-8244, 1944-8252 URL https://pubs.acs.org/doi/10.1021/acsami.9b08854

[27] Hauder M, Gstöttner J, Hansch W and Schmitt-Landsiedel D 2001 *Applied Physics Letters* **78** 838–840

[28] Chavez K L and Hess D W 2001 *Journal of The Electrochemical Society* **148** G640 ISSN 00134651 URL https://iopscience.iop.org/article/10.1149/1.1409400

[29] Berg S, Kutra D, Kroeger T, Straehle C N, Kausler B X, Haubold C, Schiegg M, Ales J, Beier T, Rudy M, Eren K, Cervantes J I, Xu B, Beuttenmueller F, Wolny A, Zhang C, Koethe U, Hamprecht F A and Kreshuk A 2019 *Nature Methods* ISSN 1548-7105 URL https://doi.org/10.1038/s41592-019-0582-9

[30] Wallenberger F and Bingham P 2009 *Fiberglass and Glass Technology: Energy-friendly Compositions and Applications* (Springer US) ISBN 978-1-4419-0736-3

[31] Baer D R and Sherwood P M A 2025 *Frontiers in Analytical Science* **4** 1509438 ISSN 2673-9283 URL https://www.frontiersin.org/articles/10.3389/frans.2024.1509438/full

[32] Li D, Chen Y, Zhou C, Shi C, Xu Z, Miao Z, Xi Z and Han J 2024 *Materials Chemistry Frontiers* **8** 715–731 ISSN 2052-1537 URL https://xlink.rsc.org/?DOI=D3QM01036H

[33] IPC (Organisation) and Task Group (7-31b) 2020 *IPC-A-610G Acceptability of Electronic Assemblies* (IPC-Association Connecting Electronics Industries) ISBN 978-1-951577-61-2

[34] Hillman D, Pearson T and Coyle R 2024 *Journal of Surface Mount Technology* **37** 19–33

[35] Vianco P and Society A W 1999 *Soldering Handbook* (American Welding Society) ISBN 978-0-87171-618-7

[36] Perdigones F and Quero J 2022 *Micromachines* **13** 460

[37] Graves A and Qualmann K 2018 *The Science of Baking Soda* (ACS Axial) URL https://axial.acs.org/cross-disciplinary-concepts/the-science ...

[38] Waple B 2017 *Restoration & Remediation* **2**